



<http://www.diva-portal.org>

Preprint

This is the submitted version of a paper published in *Journal of Chemical Theory and Computation*.

Citation for the original published paper (version of record):

Zheng, G., Witek, H A., Bobadova-Parvanova, P., Irle, S., Musaev, D G. et al. (2007)
Parameter calibration of transition-metal elements for the spin-polarized self-consistent-charge density-functional tight-binding (DFTB) method: Sc, Ti, Fe, Co, and Ni.
Journal of Chemical Theory and Computation, 3(4): 1349-1367
<http://dx.doi.org/10.1021/ct600312f>

Access to the published version may require subscription.

N.B. When citing this work, cite the original published paper.

Permanent link to this version:

<http://urn.kb.se/resolve?urn=urn:nbn:se:uu:diva-145477>

**Parameterization of Transition Metal Elements for the Spin-Polarized
Self-Consistent-Charge Density-Functional Tight-Binding (DFTB) Method:
Parameterization of Sc, Ti, Fe, Co, and Ni**

Guishan Zheng,¹ Henryk Witek,² Petia Bobadova-Parvanova, Stephan Irle,³
Djamaladdin G. Musaev, Rajeev Prabhakar,⁴ and Keiji Morokuma*
*Department of Chemistry and Cherry L. Emerson Center for Scientific Computation,
Emory University, Atlanta, Georgia 30322*
and
Marcus Elstner,⁵ Christof Köhler[¶] and Thomas Frauenheim[¶]
Universität Paderborn, Fachbereich Physik, 33095 Paderborn, Germany

Abstract: Parameters were developed for five first-row transition metal elements (M=Sc, Ti, Fe, Co, and Ni) in combination with H, C, N, O as well as the same metal (M-M) using the spin-polarized self-consistent-charge density-functional tight-binding (DFTB) method. To test their performance a couple sets of compounds have been selected to represent a variety of interactions and bonding schemes that occur frequently in transition metal containing systems. The results show that the DFTB method with the present parameters in most cases reproduces structural properties very well but the relative energies of different spin states only qualitatively compared to the B3LYP/SDD+6-31G(d) density functional (DFT) results.

¹ Present address: Department of Chemistry, University of Illinois, Urbana, IL 61801

² Present Address: Institute of Molecular Science and Department of Applied Chemistry, National Chiao Tung University, Hsinchu, Taiwan

³ Present Address: Fukui Institute for Fundamental Chemistry, Kyoto University, Sakyo, Kyoto 606-8103, Japan

⁴ Present Address: Department of Chemistry, University of Miami, Coral Gables, FL 33124

* The corresponding author. email: morokuma@emory.edu. Also at Fukui Institute for Fundamental Chemistry, Kyoto University, Kyoto, Japan

⁵ Present Address: Technical University, Braunschweig, Germany

[¶] Present Address: University of Bremen, Bremen, Germany

1. INTRODUCTION.

Molecules that contain transition metal atoms play an important role in catalysis, material science, drug design, and enzymatic reactions. Theoretical modeling of such systems is challenging due to their large size and complexity of their electronic structure arising from the presence of chemically active d-electrons. Despite the advent of fast computers and advanced techniques, high level *ab initio* methods are prohibitively expensive to treat very large molecular systems. A partial remedy for this problem can be the density functional theory (DFT),¹ which can be used routinely to systems containing a few hundred atoms with the present computers.

Efforts to reduce computational cost associated with quantum chemical calculations have led in last several decades to development of a large number of semiempirical methods, such as MNDO,² SINDO/1,³ AM1,⁴ PM3,⁵ SAM1,⁶ MNDO/d,⁷ PM3/tm,⁸ and NDDO-G,⁹ which can routinely treat molecular systems containing up to a thousand or so atoms. An alternative approach to perform calculations for such large systems is an approximate density functional technique called the density functional tight-binding (DFTB) method.^{10,11} This method has been applied to calculating energies, geometries and spectra of organic and inorganic molecules,¹⁰⁻¹⁴ The accuracy for molecular geometries is comparable to that of DFT-GGA methods, while reaction energies and vibrational frequencies are slightly less accurate. Recently, a special parameterization for vibrational frequencies has shown that DFTB can approach the DFT accuracy,¹⁵ while heats of formation are still slightly less accurate than those determined at recently optimized MNDO approaches.¹⁶

In the present article, we will use a specific version of the series of DFTB methods, the spin-polarized self-consistent charge DFTB,¹⁸ which is based on a second-order expansion of the Kohn-Sham total energy with respect to spin densities. This method introduces a self-consistent-charge (SCC) calculation of the spin density using Mulliken populations. The SCF procedure minimizes the dependence of the results on the choice of the zero-order initial density, and substantially increases the transferability of the parameters in comparison with the non-self-consistent-charge approach.¹¹ In addition, the spin-polarized version of DFTB

distinguishes different spin distributions (whereas spin-unpolarized DFTB depends only on the total electron density) and can qualitatively describe different spin states, a fact that is essential for transition metal elements. All the needed one- and two-center integrals are pre-computed for a large number of grid points, and in practical calculations, the actual values of integrals are obtained by a suitable interpolation scheme, usually a cubic spline function fitting. All parameters of the spin-polarized DFTB model are calculated from DFT using the PBE functional; no fitting to experimental data is involved. Since only valence electrons are considered in a minimal basis set and explicit integral evaluations are not required, DFTB is computationally comparable to semiempirical methods (like MNDO, AM1, PM3) and two to three orders of magnitude faster than *ab initio* Hartree-Fock (HF) and density functional theory (DFT) methods.¹² As a result, the computational speed of DFTB is determined to a large extent by the solution of the generalized eigenvalue problem.

Up to now, the only transition metals available in DFTB were Zn¹³, Au,¹⁴ and some other scattered atom pair parameters,¹⁷ and therefore one of the serious drawbacks of the DFTB method was the lack of parameters for further transition metal elements, which play an important role in many inorganic, organometallic and metalloprotein problems.. This situation has restricted the active use of DFTB methods from many interesting applications.

In the present paper, we present our recent work on extending the currently available spin-polarized DFTB parameter database in the form of the Paderborn group to five additional elements: Sc, Ti, Fe, Co, and Ni, which are parameterized in combination with C, H, O, and N non-metal elements as well as with the element itself (dimer). In Section 2, we give an overview of our parameterization procedure. In Section 3, the details of actual computations are presented, and in Section 4, test calculations using the new parameters are discussed and analyzed. Here, the performance of the parameter sets in different chemical environments is discussed in detail, focusing on calculated molecular geometries and relative energies. In the last Section, we summarize the performance and problems of the new parameters.

2. METHOD AND PARAMETERIZATION

A. Spin-Polarized Self-Consistent-Charge DFTB Approach

A detailed description of the spin-polarized self-consistent-charge density-functional tight-binding (DFTB) method has been given elsewhere.^{18,19,20} Here a brief review is presented.

The total spin-polarized DFTB energy is given by

$$E_{\text{tot}}^{\text{SDFTB}} = \sum_{\sigma=\uparrow,\downarrow} \sum_i^{\text{MO}} n_i^\sigma \langle \psi_i^\sigma | \hat{H}^0[\rho_0] | \psi_i^\sigma \rangle + \frac{1}{2} \sum_{A,B}^{\text{atom}} \gamma_{AB} \Delta q_A \Delta q_B + \frac{1}{2} \sum_A^{\text{atom}} \sum_l \sum_{l'} p_{Al} p_{Al'} W_{All'} + E^{\text{rep}}, \quad (1)$$

where \uparrow and \downarrow denote the up and down spin orientation, γ_{AB} is a distance-dependent interaction parameter between induced Mulliken charges $\Delta q_A, \Delta q_B$ on atoms A and B , $W_{All'}$ is a one-center interaction parameter between the l and l' shell spin densities $p_{Al}, p_{Al'}$ on atom A , E_{rep} is a sum of two-center core-core repulsive potentials:

$$E^{\text{rep}} = \sum_{A<B}^{\text{atom}} E_{AB}^{\text{rep}} \quad (2)$$

and n_i^σ is the occupation number of the spinorbital ψ_i^σ that is given as a linear combination of localized pseudo-atomic Slater orbitals χ_μ

$$\psi_i^\sigma = \sum_\mu^{\text{AO}} c_{\mu i}^\sigma \chi_\mu. \quad (3)$$

The induced Mulliken charge Δq_A on atom A is given by

$$\Delta q_A = \sum_i^{\text{MO}} \sum_{\mu \in A} \sum_v^{\text{AO}} \left(n_i^\uparrow c_{\mu i}^\uparrow c_{vi}^\uparrow + n_i^\downarrow c_{\mu i}^\downarrow c_{vi}^\downarrow \right) S_{\mu v} - q_A^0 \quad (4)$$

and the spin density p_{Al} of shell l on atom A is given by

$$p_{Al} = \sum_i^{\text{MO}} \sum_{\mu \in l, A} \sum_v^{\text{AO}} \left(n_i^\uparrow c_{\mu i}^\uparrow c_{vi}^\uparrow - n_i^\downarrow c_{\mu i}^\downarrow c_{vi}^\downarrow \right) S_{\mu v}, \quad (5)$$

where S is the overlap matrix of pseudo-atomic Slater orbitals and q_A^0 is the valence charge on the neutral atom A . The effective Kohn-Sham Hamiltonian \hat{H}^0 depends only on the reference density ρ_0 .

The derivation of the spin-polarized DFTB energy with respect to nuclear coordinate a yields the DFTB energy gradient acting on atom A. The exact formula and its derivation can be found elsewhere.²⁰

B. Development of Atomic and Diatomic Parameters Sets

We develop the M-M and M-X diatomic parameter sets, where M = Sc, Ti, Fe, Co, Ni, and X = H, C, O, N. Atomic valence orbitals are obtained by solving an all-electron Kohn-Sham atomic eigenvalue problem with an additional confining potential. The repulsive potentials for each pair of atoms are obtained by reproducing DFT energies and geometries for a number of carefully selected molecular systems; their choice is ideally meant to represent the most important chemical compounds created by a given pair of atoms.

In the present paper, spin-polarized DFTB parameterization is performed in the same way as in the standard, non-spin-polarized self-consistent-charge (SCC-) method.²¹ Here, we will review briefly the main ideas of the parameterization procedure together with necessary modifications required by the introduction of the spin-polarization term. There are two families of parameters necessary to construct the spin-polarized DFTB Hamiltonian, namely 1) atomic parameters obtained from calculations for confined pseudo-atoms, and 2) diatomic distance-dependent parameters obtained from diatomic calculations.

Atomic Parameters. The required spin-polarized DFTB atomic parameters comprise atomic basis functions χ_a , atomic reference densities ρ_0 , chemical hardness or Hubbard parameters U_{Al} , and the atomic spin-dependent constants W_{All} . U_{Al} is determined by taking the second derivative of the total atomic energy with respect to the total charge on orbital l of atom A. The values of W_{All} are calculated by taking the second derivatives of total atomic energy with respect to the spin density; at the point where the spin density is zero, this derivative reduces to:¹⁸

$$W_{All} = \frac{1}{2} \left(\frac{\partial \epsilon_{Al}^\uparrow}{\partial n_l^\uparrow} - \frac{\partial \epsilon_{Al}^\downarrow}{\partial n_l^\downarrow} \right)_{\rho=0} = W_{Al'l} \quad (6)$$

where n_l and $n_{l'}$ are the occupation numbers of atomic shells l and l' , respectively, and $\varepsilon_{Al}^\uparrow$ is the atomic Kohn-Sham orbital energy for alpha (\uparrow) spin. The determined values of U_{Al} and W_{Al} are listed in Table 1 for all the considered metal elements.

We use a standard procedure to construct the atomic basis set. It is expressed as a linear combination of Slater spherical harmonics; the coefficients are obtained from atomic Kohn-Sham calculations with the PBE functional²² and an additional confining potential $(r/r_0)^2$ (in Hartree). The confinement mimics the behavior of atoms in molecular systems and in solids. The values of r_0 (4.86 for Sc, 3.6 for Ti, 3.2 for Fe, 4.38 for Co and 3.2 for Ni, all in bohr) have been selected out of a large number of trials and ensure that SCC-DFTB reproduces accurate DFT electronic band structures for solid state metals to the highest possible degree.

Diatomic Parameters. The overlap $S_{\mu\nu}$ and Hamiltonian $H_{\mu\nu}^0$ matrix elements are obtained from two-center approximate DFT calculations on the corresponding diatomic compounds for a large number of different interatomic distances, i.e. the two-center integral calculations using atomic wavefunctions from previous pseudoatomic calculations. The term “approximate DFT” refers to the fact that exchange-correlation functional is built from approximate electronic density obtained as a simple sum of unperturbed atomic densities. The atomic densities for these transition metal atoms are obtained from an auxiliary pseudoatomic calculation with an additional confining potential $(r/r_0)^2$, where a universal value of $r_0=14$ bohr is adopted for all studied transition metals. It is important to stress that the confinement radius r_0 used previously to construct valence atomic orbitals is different from the confinement radius used here to generate the zero-order unperturbed atomic density. The confinement radius for the orbitals is used to generate a minimal LCAO basis set that is appropriate for the target molecular systems, i.e. the choice of this parameter for the basis set determination can be compared to procedure of basis set construction for HF or DFT calculations and r_0 has originally been treated as a variational parameter.²³ The choice of the confinement radius for the density is different in its nature; it can be interpreted as an empirical value to generate an optimal starting (input) density that is characteristic to tight-binding methods.²⁴

These two confinement radii can be treated as parameters used to enhance the performance of new DFTB parameter sets. However, the influence of these values on molecular properties is rather small. In the present parameterization procedure the PBE functional is used.²² The orbitals employed in this calculation are atomic Slater orbitals with confined potential discussed in the paragraph above. The values of $S_{\mu\nu}$ and $H_{\mu\nu}^0$ are represented numerically on a grid of atomic distance.

Determination of the two-center repulsive potentials E_{AB}^{rep} is the most labor-intensive and therefore most time-consuming step in the parameterization procedure. The repulsive potential function is the difference between the DFT energy and the DFTB electronic energy as a function of atomic distance. At first, segments of each repulsion potential were calculated for a carefully selected group of molecules (called Tier 1 molecules in Table 2) representing a large spectrum of bonding situations (covalent single and multiple bonds, ionic bonds, back-donation bonds, π -interactions, etc.) for a given pair of elements A-B. We have used small molecules containing only few atoms, in which typically additional hydrogen or other atoms have been used to saturate the unfilled valences of given transition metal and non-metal atoms. In general, mainly closed-shell molecules have been used at this stage of the parameterization to avoid additional complication; however, in certain cases, some open-shell molecules have also been included. Following the standard DFTB parameterization procedure, the thereby determined segments of the two-center repulsive potentials were connected to yield a continuous curve $E_{AB}^{\text{rep}}(R)$ that was shifted up or down in energy so that the DFTB energetics of the larger test molecules (called Tier 2) and also in some cases for some Tier 3 molecules (see the next section for their definition) reasonably reproduces that of the DFT benchmark calculations at the B3LYP/SDD+6-31G(d) level (see the next Section for definition of the basis set). Since $E_{AB}^{\text{rep}}(R)$ has to be zero at $R=\infty$, the $E_{AB}^{\text{rep}}(R)$ curve determined above was extrapolated smoothly to zero as R becomes large. The choice of various test molecules as well as the amount of the repulsion potential shift and the way of extrapolation are “empirical” procedures to determine the

reliability of the DFTB parameters.

In the standard DFTB parameterization procedure all the two center parameters, i. e. the overlap $S_{\mu\nu}$ and Hamiltonian $H_{\mu\nu}^0$ matrix elements between a set of valence orbitals μ and ν , as well as the charge-charge interaction parameter γ_{AB} and the core-core repulsion E_{AB}^{rep} between the two atomic centers A and B, are given in tables as functions of interatomic distances. In the present work, however, we represented them all in analytical forms which are linear combinations of exponential functions with geometric series of exponents:

$$f(R) = \sum_{k=1}^N A_k \exp(-\alpha\beta^{k-1}R) \quad (7)$$

The number of terms N and values of α , β and A_k ($k=1, N$) are fitting parameters and are given in the Supporting Information for each pairs of orbitals or atoms. The advantages of the analytical forms over the tables are: 1. The size of entry data is smaller, and 2. Functions are smooth. The second point is particularly important when derivatives of $f(R)$ with respect to R are taken for gradients and higher derivatives.

Following the procedure outlined above, we have developed new spin-polarized DFTB parameters for transition metal compounds containing Sc, Ti, Fe, Co, or Ni in combination with C, H, N, and O non-metal elements as well as with themselves.

C. Tests of Determined Parameters.

The newly developed parameter sets (used together with the DFTB parameters determined previously for the C, H, N, and O set) are tested against DFT results for a set of relatively small (called Tier 3) molecules as well as larger, more realistic (Tier 4) molecules. In the Tier 3 set of molecules, we include strongly bonded small molecules as well as weakly bonded complexes. Some of these molecules are only hypothetical and are not known experimentally. In Tier 4, larger compounds that are of greater interest for practical chemistry applications are chosen. Details concerning Tier 4 molecules are given in each of the sections dealing with the individual metal atoms. Schematic structures of the molecule sets in Tier 3 and Tier 4 are

presented in Scheme 1 and Figures 1, 2, 3 and 4. Benchmark DFT calculations are carried out with the B3LYP functional with a mixed basis set, Stuttgart/Dresden *ab initio* pseudopotential and (8s7p6d1f)/[6s5p3d1f] Gaussian valence basis set (SDD)²⁵ for transition metal elements and the popular 6-31G(d) basis set for H, C, N, and O, unless otherwise noted. The mixed basis sets will be denoted as SDD+6-31G(d) in the remainder of this work. All DFT geometry optimizations have been performed using the Gaussian03²⁶ suite of programs, and the DFTB geometry optimizations were carried out using our own DFTB code.¹⁸ Default values for gradient and displacement convergence criteria were applied throughout.

3. RESULTS AND DISCUSSIONS

In this section we test the ability of DFTB using the presently developed parameters to reproduce common DFT (namely B3LYP/SDD+6-31G(d)) results, such as bond lengths, angles, and relative energetics. We emphasize that it is not a purpose of the present paper to discuss the ability of spin-polarized DFTB to reproduce experimental results, but rather to investigate how far the approximations introduced in DFTB cause deviations from the benchmark DFT calculations. Therefore, available literature data on test molecules will not be discussed. We will only check the performance of DFTB based on the results compared with those at the B3LYP/SDD+6-31G(d) level (hereafter this level is simply called as DFT), unless otherwise noted. This was also the method used for evaluating the repulsive diatomic DFTB potentials. We compare the bond distances and angles for Tier 3 molecules, as well as the relative energies of low lying spin states, since these are very important for transition metal complexes. We did not compare simple bond dissociation energies such that $R_nM-XR'_m$, because often single-determinantal wave functions give incorrect spin states and make the direct energy comparison difficult.

A. Scandium

We present the geometrical parameters of Sc-containing Tier 3 molecules in Table 3 for

DFT and DFTB, as well as the respective difference between the two levels of theory. We have dropped Sc_2O_x systems entirely as it was impossible to converge to proper wavefunctions and geometries. The absolute average bond distance difference for Sc-Sc is 0.17 Å (0.09 Å excluding very long distance in triplet $\text{Sc}_2(\text{CH}_3)_4$), Sc-H is 0.02 Å, for Sc-C 0.06 Å, for Sc-N 0.03 Å and for Sc-O 0.03 Å. Sc-X bond lengths are therefore well described by the DFTB method with our parameters. Bond angle differences between DFT and DFTB results are on the absolute average 7.5° for Sc-Sc, 4.2° for Sc-H, 13.3° for Sc-C, 3.6° for Sc-N, and 28.4° for Sc-O. These deviations are generally much smaller than those we encountered for more d-electron rich transition metal elements, further described below, indicating a better performance of the DFTB method when fewer d-electrons are present. The large discrepancy for the O-Sc-O bond in the quartet state of the ScO_2 molecule with 43.7° is an exception; because of the lack of more angle parameters, the average absolute value of Sc-O angle deviations is large. The overall average absolute bond distance difference between DFTB and DFT is 0.04 Å, the overall average absolute bond angle difference is 12.4°. Therefore, generally speaking, DFTB geometries are in reasonable agreement with those predicted by DFT.

In Table 4 the relative energies of high spin and low spin states of Sc-containing molecules are shown. The DFT energy orders are reproduced by DFTB except for Sc_2H and $\text{Sc}^+(\eta^2\text{-N}_2)$, where state splittings are relatively small. Although the magnitude of state splitting difference between DFT and DFTB can be as large as 38 kcal/mol (in the case of Sc_2H), the average absolute differences between DFT and DFTB state splitting energies are 13.1 kcal/mol for Sc-Sc, compounds, 14.2 kcal/mol for Sc-H, 14.0 kcal/mol for Sc-C, 18.1 kcal/mol for Sc-N, and 15.4 kcal/mol for Sc-O compounds. This performance is better than for d-electron rich transition metal elements, as we already noted for geometries. The overall average deviation is 15.1 kcal/mol. We report an overall tendency in DFTB to overestimate the binding energies of low spin complexes. Consequently, DFTB energetics should be carefully checked in the case of scandium parameters, but are more reliable in general than for d-electron rich elements (see

below).

As an example of Tier 4 molecule, in Figure 1, we compare B3LYP/6-311+G(d) geometries and energies of linear $\text{Sc}(\text{CC})_n$ ($n=1, 2, 3, 4$) in their electronic ^2S ground states with the corresponding DFTB results. The DFT results were already partially presented by Redondo *et al.*²⁷ who however did not provide the Sc-C binding energies for this series of polyynes chains. As one can see, DFTB structural results are in reasonable agreement with the B3LYP calculations, with bond differences largest for the Sc-C bond. Here, DFTB gives bond lengths that are too long by up to 0.08 Å. As for the C-C bond lengths, the DFTB values are consistently longer compared to the B3LYP/6-311+G(d) results for both short/long alternating bond types. Energetics is in excellent agreement, with DFTB overbinding by only 3 kcal/mol, except for the special case of ScC_2 where DFTB underbinds by about 10 kcal/mol in this most strongly bound species due to the overstabilization of the C_2 unit.

B. Titanium

As shown in Table 5, the present set of Ti DFTB spin-polarized parameters leads to optimized geometries close to those obtained by DFT. The average absolute deviations between bond lengths obtained by DFT and DFTB are 0.05 Å for Ti-H, 0.06 Å for Ti-C, 0.02 Å for Ti-N, and 0.03 Å for Ti-O, respectively. Also, bond angles are reasonably described by DFTB when compared with those obtained by DFT, with the average deviation of angles for all Tier 3 molecules studied here being 7.0°. However, individual angular deviations can be quite large, for instance the deviation of DFTB Ti-H-Ti angle from the DFT angle in Ti_2H is 37.4°, leading to a too strongly bent DFTB structure in this case. Other Ti-H-Ti angles are described much better and their deviations range from 0° to about 15°, following no obvious trend of either too sharp or too flat angles. The same holds true for Ti-X-Ti and X-Ti-X angles with X=C, N, and O, with the only exception of $\text{Ti}(\text{O}_2)$. In this T-shaped molecule, the main failure lies in the underestimated Ti-O bond distance in DFTB, leading to a too sharp O-Ti-O angle. Problems of DFTB with the Ti-O parameter sets obviously are encountered for such polar Ti π -complexes,

which is not surprising considering the fact that Tier 1 and Tier 2 molecule sets did not include such weak bonding situations. Overall, the performance of our Ti parameters for DFTB optimized geometries is very reasonable, especially given the fact that change of basis sets and density functionals can result in similar deviations among DFT calculations. Therefore, we conclude that the geometry performance of DFTB is acceptable for the Ti-X systems.

Relative energies (relative to the respective high-spin states) of the lower-lying electronic states of Tier 3 Ti-containing molecules for DFT and DFTB as well as the absolute deviation between relative energies for the two respective methods are given in Table 6. The relative energy order between high and low spin states predicted by DFT is reproduced by DFTB in most cases. However, the difference between DFTB and DFT relative energies can be as large as 25 kcal/mol, as was encountered for the TiO molecule where the low spin state is appreciably overstabilized in the DFTB method. Partially this difference can be explained by the well-known fact that B3LYP shows a preference for the high spin state due to the inclusion of exact Hartree-Fock exchange, whereas spin-dependent atomic parameters in DFTB are derived from the non-hybrid PBE density functional. A similar tendency for low spin state stabilization is also seen in case of the molecules Ti_2H_2 , Ti_2H and $\text{Ti}(\text{C}_2\text{H}_4)^+$, where the B3LYP high spin states are actually lower in energy than the respective low-spin states, while DFTB predicts a reverse energetic ordering. However, these molecules feature relatively small spin state splittings in DFT (smaller than 10 kcal/mol), and the sign change in DFTB is therefore within the average absolute deviation of 13.7 kcal/mol. Therefore we conclude that DFTB predicts the relative energy order between high- and low-spin states in most cases reasonably well.

As to a Tier 4 system, we tested one specific reaction $[(\text{Cp}-\text{CH}_2-\text{Cp})\text{TiCH}_3]^+ + \text{C}_2\text{H}_4 \rightarrow [(\text{Cp}-\text{CH}_2-\text{Cp})\text{Ti}(\text{CH}_2\text{CH}_2\text{CH}_3)]^+$ exemplifying a polymerization processes involving a Ti catalyst. DFT and DFTB geometries as well as respective energetics are presented in Figure 2. In this “real-life” scenario, again we find that DFT geometries of Ti-containing species are reasonably well reproduced by DFTB with bond length differences of at most about 0.1 Å.

However, the relative stability of these complexes as predicted by DFT is not reproduced by DFTB, which shows a strong tendency to overbinding of ethylene and results in smearing out subtle energetic differences of a few kcal/mol between isomeric complexes that are predicted by DFT. This finding shows that DFTB binding energies are not as reliable as geometrical parameters, and have to be used with great caution.

C. Iron

In Table 7, the geometries of Tier 3 molecules optimized at DFT and DFTB levels are listed. The average absolute deviation of DFTB results from DFT is 0.09 Å for Fe-H bond distance, 0.08 Å for Fe-C, 0.10 Å for Fe-N, and 0.06 Å for Fe-O. These values are again within 0.1 Å, which we consider to be acceptable, considering comparable geometrical changes introduced by the change of basis set and/or density functional for DFT calculations. Bond angles perform better for X-Fe-X and Fe-X-Fe than for the corresponding Ti systems, with average absolute deviations of 9.6° for Fe-H, 6.5° for Fe-C, 12.9° for Fe-N, and 11.2° for Fe-O systems. The largest deviations in bond angles are actually found for Fe(NH₂)₂ and FeO₂ systems with about 30°. For these compounds, qualitatively different geometries are predicted by DFTB when compared to DFT (bent structure vs. linear or vice versa). This difference may stem from the fact that in DFTB parameterization the d⁷s¹ configuration is used, which prefers linear structure arising from sd hybridization. Concerning the overall performance of DFTB for geometrical parameters however, we find that bond distances and angles of DFT geometries are typically well reproduced by DFTB.

The relative energies between different spin states of the Fe-containing Tier 3 molecules are shown in Table 8. DFTB predicts usually the same energetic order as the one computed by DFT. Fe₂H, FeO, FeO₂, Fe(O₂), and Fe₂O₄ molecules are exception to this rule with reversed energy order of low and high-spin states. Similarly to Ti, B3LYP generally favors high-spin states when compared with the DFTB approach. This is however not true for all cases; for instance, the quartet state of Fe(η²-N₂) is 38.3 kcal/mol lower in energy relative to the doublet state in

DFTB than in DFT. In general, relative energy differences between high spin state and low spin state between DFT and DFTB can be as large as 40 kcal/mol.

As a Tier 4 molecule, binding of CO to heme molecule with an axial histidine residue has been investigated. The structure of this complex is shown in Figure 3. The DFT geometry is well reproduced by DFTB. The only exceptions are the Fe-N_{imidazole} and Fe-C distance trans to Fe-N_{imidazole}, which are 0.44 Å too long and 0.12 Å too short, respectively, in DFTB. The computed binding energy of CO is 55.7 kcal/mol for DFT, while for DFTB it is only 26.5 kcal/mol despite the short Fe-CO distance. This is in contrast to the case of π and σ bonding of ethylene to a Ti complex discussed above, where DFTB predicts generally too large binding energies. Again, DFTB energetics may have to be used with great caution.

D. Cobalt

The structural parameters of Co-containing Tier 3 molecules for both DFT as well as DFTB and the respective relative differences are listed in Table 9. As observed for the cases of Sc, Ti and Fe, the Co DFTB geometries are in good agreement with DFT optimized structures. Compared with DFT results, the average absolute deviation of bond distance is 0.04 Å for Co-H, 0.06 Å for Co-C, 0.03 Å for Co-N, and 0.01 Å for Co-O. For bond angles, the average absolute deviation of DFTB from DFT is 5.0° for Co-H parameters, 5.7° for Co-C, 9.9° for Co-N, and 6.9° for Co-O. Some linear structures are preferred in DFTB results presumably due to d^8s^1 Co atomic configuration used in parameterization, a phenomenon described above for Fe. Yet, X-Co-X and Co-X-Co angles are generally in better agreement with DFT structural parameters than for corresponding Fe and Ti systems. We cannot comment at this stage on the origin of this exceptional good performance of Co DFTB parameters. Overall, from the average deviation values discussed above, we conclude that DFTB very reasonably reproduces DFT geometries in the case of Co-containing compounds.

The relative energy order between high spin and low spin states for different Co containing molecules are summarized in Table 10. The relative energy orders in DFT are well reproduced

by DFTB except CoH_2 , $\text{Co}(\text{CH}_3)_2$, $\text{CpCo}(\text{C}_2\text{H}_4)^+$, CoCp^+ and $\text{Co}(\text{NH}_2)_2$. Considering their high spin states are favored by B3LYP, DFTB reasonably predict the relative energy order although the absolute values deviation is 20.7 kcal/mol on the average, with the largest difference being about 54 kcal/mol in the case of CoCp^+ . Particularly noticeable is the DFTB preference for low-spin states in the case of Co-C systems, but noticeable exceptions from this rule exist, for instance Co_2H_4 , where DFTB favors the high-spin state by 21 kcal/mol relative to DFT.

As a real case Tier 4 system, binding of adenosyl and methyl groups, respectively, to cobalamin has been investigated. The molecular structures of adenosylcobalamin and methylcobalamin are shown in Figure 4. The geometries in both structures are well described by DFTB compared with the corresponding structures from DFT. The largest bond distance difference is about 0.18 Å in only one case. Again, DFTB predicts Co-N bond distance orders correctly. The binding energy of the adenosyl group to cobalamin is 70.3 kcal/mol in DFTB, that is 12.5 kcal/mol higher in comparison to 57.8 kcal/mol in DFT. Similarly, the binding energy of the methyl group to cobalamin is 94.3 kcal/mol in DFTB, that is an overbinding of 22.2 kcal/mol when compared to 72.1 kcal/mol in DFT. Thus, it is concluded that DFTB performs well in terms of geometries. Again we should caution about the use of DFTB for the prediction of energetics due to the unforeseeable over- or underbinding errors.

E. Nickel

The geometrical parameters of Ni-containing Tier 3 molecules are shown in Table 11 for DFT and DFTB, as well as the respective difference between the two levels of theory. In the case of triplet $\text{Ni}_2(\text{CH}_3)_4$, DFT predicts an asymmetric structure with one bridging methyl group, whereas the DFTB triplet geometry resembles more closely the symmetric DFTB singlet geometry. The average absolute bond distance difference is 0.15 Å for Ni-Ni, 0.06 Å for Ni-H, 0.19 Å for Ni-C, 0.04 Å for Ni-N and 0.02 Å for Ni-O. The Ni-C distance is not well described in cases where cyclopentadienyl (Cp) rings interact with Ni. Here, Ni-C bonds are typically too long by a few tenths of an angstrom, mainly because the position of the Ni on top of the Cp

system is very flexible. Bond angle differences between DFT and DFTB results are on the absolute average 16.2° for Ni-Ni, 12.2° for Ni-H, 18.8° for Ni-C, 30.8° for Ni-N, and 7.7° for Ni-O. The rather large deviations are a consequence of the fact that DFTB very often prefers linear arrangements, when the lowest DFT structure is bent (as seen also for Fe and Co above). The overall average absolute bond distance difference between DFTB and DFT is 0.09 Å, the overall average bond angle difference is 17.1°. Therefore, more generally speaking, DFTB geometries are in reasonable agreement with those predicted by DFT, which is consistent with the findings in the case of other transition metal elements in this work.

In Table 12, the relative energies of high spin and low spin states of Ni-containing molecules are shown. The DFT energy orders are reproduced by DFTB except for Ni₂H₂, NiCp⁺, Ni(NH₂)₂⁺, NiO₂, and Ni(O₂), where state splittings are generally very small. However, the magnitude of state splitting difference between DFT and DFTB can be as large as 50 kcal/mol (in the case of Ni₂H₄). Average absolute differences between DFT and DFTB state splitting energies are 32.4 kcal/mol for Ni-H, 14.9 kcal/mol for Ni-C, 19.8 kcal/mol for Ni-N, and 20.6 kcal/mol for Ni-O. The overall average absolute deviation is 21.9 kcal/mol. Again we report an overall tendency in DFTB to overestimate the binding energies of low spin complexes. Consequently, DFTB energetics should be carefully checked in the case of nickel parameters as well.

In Figure 5, as an example of real case Tier 4 system, structures and energetics of the intermediates of ethylene insertion step of [C₂H₄N₂NiCH₃]⁺ + C₂H₄ → [C₂H₄N₂NiCH₂CH₂CH₃]⁺ are presented. DFT geometries and energetics at the B3LYP/Lanl2DZ level were taken from reference.²⁸ This system features Ni-H, Ni-C, and Ni-N interactions and similar trends as found for molecules in Table 11 can be observed. Ni-X bond lengths are generally too long by about 0.1 Å (with some exceptions). An exception is a very long agostic Ni···H distance of 2.72 Å for DFTB as compared to 2.15 Å for DFT the γ-complex; such a weak interaction does not seem to be properly parameterized. Energetically, DFTB interaction energies for π- and γ-complexes are in almost perfect agreement with DFT, but the β-complex is severely underbound relative to the

γ -complex, which is in stark contrast to the DFT results. This finding underlines once again that energetics obtained at the DFTB level of theory are to be trusted only with great caution.

4. SUMMARY AND CONCLUSIONS

From the above given discussions in which geometries and energetics of Tier 3 and Tier 4 molecules were presented for each transition metal element at both the B3LYP/SDD+6-31G(d) as well as spin-polarized DFTB level of theory, we can make the following summary:

1. Spin-polarized DFTB with the present parameters for transition metal elements Sc, Ti, Fe, Co and Ni in combination with H, C, O, N and same-element bonding partners reproduce B3LYP/SDD+6-31G(d) geometries reasonable well, both bond distances (average absolute differences mostly below 0.1 Å) as well as angles (average absolute deviations between 10° and 20°) except for cases where DFTB noticeably prefers linear bond environments, presumably as a consequence of the atomic DFTB parameter evaluation. Problems also occur in bonding situations where particular bond types were not included in Tier 1 and Tier 2 molecule sets, such as metal-nonmetal π -bonds. A remedy of this problem would obviously involve the inclusion of π -complexes in Tier 1 and 2 sets of molecules; however the overall DFTB performance for geometrical parameters is likely to suffer in such a case.

2. For the energy differences between different spin states of Tier 3 molecules, spin-polarized DFTB energetic orders qualitatively agree with DFT in most cases. However, for quantitative comparison, there are cases of both over- as well as underbinding by as much as 50 kcal/mol. While DFTB shows a tendency to overestimate the stability of low-spin complexes relative to their corresponding high-spin states, we found several exceptions to this rule. For Tier 4 molecules, we also found both over- as well as underbinding situations of the order of tens of kcal/mol, making the use of DFTB predicted energetics only qualitative.

Therefore spin-polarized DFTB parameters for Sc, Ti, Fe, Ni and Co in connection to H, C, N, O and own elements should be taken as “preliminary”, with a reasonable geometrical performance but with only qualitative or “ballpark” energetic reliability and should be further

tested for individual cases.

The deficiency in energetic prediction of spin-polarized DFTB with the present transition metal parameters is expected to be greatly reduced in the ONIOM(QM:QM) scheme adopting DFTB as the low-level method. In this scheme the energetics of the “active” part will be calculated using more reliable high-level method and the energetic errors in the DFTB calculations will be mostly canceled out. Since there is virtually no reliable semiempirical method for transition metal complexes, even “preliminary” spin-polarized DFTB parameters would be useful for ONIOM(QM:QM) calculations. The use of QM as the low-level method is in some cases essential; QM methods take into account electronic effects of the environment and are fully polarizable; both of these important effects are neglected completely when standard MM is used as the low-level method. The applicability of the present transition metal parameters in the ONIOM(QM:DFTB) will be further explored in subsequent work.

In the present parameterization, we used B3LYP/SDD+6-31G(d) for the calibration of the DFTB parameters. As is well known, a weak point of the DFT method is the lack of an absolutely reliable functional. In particular, the amount of mixing of the “exact” (Hartree-Fock) exchange functional often controls the relative energies of different spin states. B3LYP has been used in the original parameterization of (H, C, N, O) set and is one of the most popular functionals in chemistry with “somehow magic” hybrid ratio. Although in many cases such hybrid functionals with a small fraction of the exact exchange are known to give reasonable relative energies of different spin states,²⁹ there are many exceptions as well. Therefore, if one tries to fit DFTB parameters to reproduce a different functional, one would result in a different parameter set.

The problems in predicting DFT-like energetics is partly stemming from the current fitting scheme for the diatomic pair repulsive curve and needs further improvement. Another problem of the present scheme of parameter determination is that one has to carefully work on each pair of elements, which is extremely time consuming; with a few element pairs a year, it will be long before one can cover all the important element pairs. A more systematic method of

determining parameters for a set of pairs of elements at the same time will be required. Efforts along these lines are in progress.

Acknowledgement. We would like to acknowledge Dr. David Quinero for his participation in the early stage of this work. This work was supported in part by grants from the U.S. National Science Foundation (CHE-0209660), U.S. Department of Energy (DE-FG02-03ER15461), Deutsche Forschungsgemeinschaft (DFG) and University of Paderborn. Computer resources were provided by the Cherry Emerson Center for Scientific Computation.

Supporting Information. The values of the SDFTB parameters determined in the present paper will be available at the following web site: <http://www.dftb.org>.

References

- ¹ P. Hohenberg and W. Kohn, *Phys. Rev.* **136**, B864 (1964); W. Kohn and L. J. Sham, *Phys. Rev.* **140**, A1133 (1965); R. G. Parr and W. Yang, *Density-Functional Theory of Atoms and Molecules*. (Oxford University Press, New York, 1989); K. Koch and M. C. Holthausen, *A Chemist's Guide to Density Functional Theory: An Introduction and Practical Guide to DFT Calculations*. (Wiley-VCH, Weinheim, 2000).
- ² M. J. S. Dewar and W. Thiel, *J. Am. Chem. Soc.* **99**, 4899 (1977); M. J. S. Dewar and W. Thiel, *J. Am. Chem. Soc.* **99**, 4907 (1977).
- ³ D. N. Nanda and K. Jug, *Theor. Chim. Acta* **57**, 95 (1980); K. Jug, R. Iert, and J. Schulz, *Int. J. Quantum Chem.* **32**, 265 (1987).
- ⁴ M. J. S. Dewar, E. Zebisch, E. F. Healy, and J. J. P. Stewart, *J. Am. Chem. Soc.* **107**, 3902 (1985).
- ⁵ J. J. P. Stewart, *J. Comput. Chem.* **10**, 209 (1989); J. J. P. Stewart, *J. Comput. Chem.* **10**, 221 (1989).
- ⁶ M. J. S. Dewar, C. Jie, and J. Yu, *Tetrahedron* **49**, 5003 (1993); A. J. Holder, R. D. Dennington, and C. Jie, *Tetrahedron* **50**, 627 (1994).
- ⁷ W. Thiel and A. A. Voityuk, *Theor. Chim. Acta* **81**, 391 (1992); W. Thiel and A. A. Voityuk, *Theor. Chim. Acta* **93**, 315 (1996).
- ⁸ SPARTAN, (Wavefunction Inc., Irvine, 1995).
- ⁹ A. A. Voityuk, M. C. Zerner, and N. Rosch, *J. Phys. Chem. A* **103**, 4553 (1999).
- ¹⁰ M. Elstner, D. Porezag, G. Jungnickel, J. Elsner, M. Haugk, T. Frauenheim, S. Suhai, and G. Seifert, *Phys. Rev. B* **58**, 7260 (1998).
- ¹¹ D. Porezag, T. Frauenheim, T. Köhler, G. Seifert, and R. Kaschner, *Phys. Rev. B* **51**, 12947 (1995).
- ¹² G. Zheng, S. Irle, and K. Morokuma, *Chem. Phys. Lett.* **412**, 210 (2005).

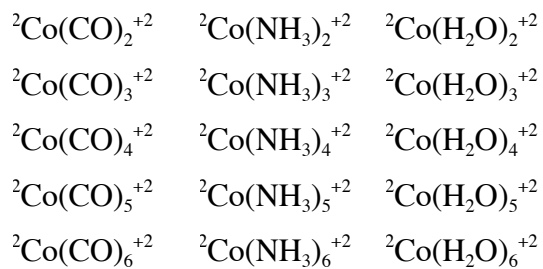
- ¹³ M. Elstner, Q. Cui, P. Muniñ, E. Kaxiras, T. Frauenheim, and M. Karplus, *J Comput Chem.* **24**, 565 (2003).
- ¹⁴ P. Koskinen, H. Häkkinen, G. Seifert, S. Sanna, T. Frauenheim, and M. Moseler, *New J. Phys.* **8**, 9 (2006).
- ¹⁵ E. Małolepsza, H. A. Witek, and K. Morokuma, *Chem. Phys. Lett.* **412**, 237 (2005).
- ¹⁶ K. W. Sattelmeyer, I. Tubert-Brohman, and W. L. Jorgensen, *J. Chem. Theo. Comp.* **2**, 413 (2006).
- ¹⁷ S. Stevenson, P. W. Fowler, T. Heine, J. C. Duchamp, G. Rice, T. Glass, K. Harich, E. Hajdu, R. Bible, and H. C. Dorn, *Nature* **408**, 427 (2000); G. Seifert, H. Terrones, M. Terrones, G. Jungnickel, and T. Frauenheim, *Phys. Chem. Chem. Phys.* **114**, 245 (2000); J.-O. Joswig, M. Springborg, and G. Seifert, *Phys. Chem. Chem. Phys.* **3**, 5130 (2001); P. Sarkar, M. Springborg, and G. Seifert, *Chem. Phys. Lett.* **405**, 103 (2005); G. Seifert, J. Tamuliene, and S. Gemming, *Comput. Mater. Sci.* **35**, 316 (2006).
- ¹⁸ C. Köhler, G. Seifert, U. Gerstmann, M. Elstner, H. Overhof, and T. Frauenheim, *Phys. Chem. Chem. Phys.* **3**, 5109 (2001).
- ¹⁹ T. Frauenheim, G. Seifert, M. Elstner, Z. Hajnal, G. Jungnickel, D. Porezag, S. Suhai, and R. Scholz, *Phys. Status Solidi (b)* **217**, 41 (2000).
- ²⁰ C. Kohler, Ph.D, University of Paderborn, 2004.
- ²¹ M. Elstner, Q. Cui, P. Muniñ, E. Kaxiras, T. Frauenheim, and M. Karplus, *J. Comput. Chem.* **24** (5), 565 (2002).
- ²² J. P. Perdew, K. Burke, and M. Ernzerhof, *Phys. Rev. Lett.* **77**, 3865 (1996).
- ²³ H. Eschrig, *The Optimized LCAO Method and Electronic Structure of Extended Systems.* (Akademieverlag, Berlin, 1988).
- ²⁴ W. Foulkes and R. Haydock, *Phys. Rev. B* **39**, 12520 (1989).
- ²⁵ M. Dolg, U. Wedig, H. Stoll, and H. Preuss, *J. Chem. Phys.* **86**, 866 (1987); U. Wedig, M. Dolg, H. Stoll, and H. Preuss, edited by A. Veillard (Reidel, Dordrecht, 1986), pp. 79.
- ²⁶ G. W. T. M. J. Frisch, H. B. Schlegel, G. E. Scuseria, M. A. Robb, J. R. Cheeseman, J. A. Montgomery, Jr., T. Vreven, K. N. Kudin, J. C. Burant, J. M. Millam, S. S. Iyengar, J. Tomasi, V. Barone, B. Mennucci, M. Cossi, G. Scalmani, N. Rega, G. A. Petersson, H. Nakatsuji, M. Hada, M. Ehara, K. Toyota, R. Fukuda, J. Hasegawa, M. Ishida, T. Nakajima, Y. Honda, O. Kitao, H. Nakai, M. Klene, X. Li, J. E. Knox, H. P. Hratchian, J. B. Cross, V. Bakken, C. Adamo, J. Jaramillo, R. Gomperts, R. E. Stratmann, O. Yazyev, A. J. Austin, R. Cammi, C. Pomelli, J. W. Ochterski, and K. M. P. Y. Ayala, G. A. Voth, P. Salvador, J. J. Dannenberg, V. G. Zakrzewski, S. Dapprich, A. D. Daniels, M. C. Strain, O. Farkas, D. K. Malick, A. D. Rabuck, K. Raghavachari, J. B. Foresman, J. V. Ortiz, Q. Cui, A. G. Baboul, S. Clifford, J. Cioslowski, B. B. Stefanov, G. Liu, A. Liashenko, P. Piskorz, I. Komaromi, R. L. Martin, D. J. Fox, T. Keith, M. A. Al-Laham, C. Y. Peng, A. Nanayakkara, M. Challacombe, P. M. W. Gill, B. Johnson, W. Chen, M. W. Wong, C. Gonzalez, and J. A. Pople, *Gaussian03 Rev. D01+* (2004).
- ²⁷ P. Redondo, C. Barrientos, and A. Largo, *J. Phys. Chem. A* **109**, 8594 (2005).
- ²⁸ D. G. Musaev, R. D. J. Froese, M. Svensson, and K. Morokuma, *J. Am. Chem. Soc.* **119**, 367 (1997).
- ²⁹ D. Quiñonero, D. G. G. Musaev, and M. Morokuma, *Inorg. Chem.* **42**, 8449 (2003); M. R. A. Blomberg, P. E. M. Siegbahn, and M. Svensson, *J. Chem. Phys.* **104**, 9546 (1996); M. Lundberg and P. E. M. Siegbahn, *J. Comp. Chem.* **26**, 661 (2005); A. Ricca and C. W. Bauschlicher, *J. Phys. Chem. A* **101**, 8949 (1997).

Table 1. Chemical hardness or Hubbard parameters U_M and the atomic spin-dependent constants $W_{Ml'}$ (both in Hartree) for $M = \text{Sc, Ti, Fe, Co}$ and Ni

Element	Sc	Ti	Fe	Co	Ni
U_s	0.188805	0.20020	0.20050	0.26064	0.23145
U_p	0.137842	0.14432	0.20050	0.11593	0.18913
U_d	0.327166	0.35522	0.36342	0.38599	0.40632
W_{ss}	-0.013	-0.014	-0.016	-0.016	-0.016
W_{sp}	-0.011	-0.011	-0.012	-0.012	-0.012
W_{sd}	-0.005	-0.004	-0.003	-0.003	-0.003
W_{pp}	-0.014	-0.014	-0.029	-0.033	-0.022
W_{pd}	-0.002	-0.002	-0.001	-0.001	-0.001
W_{dd}	-0.013	-0.014	-0.015	-0.016	-0.018

Table 2. List of molecules and their spin states used in the parameterization procedure. Tier 1 molecules are used to generate the diatomic repulsive potential curve, and Tier 2 molecules are used to adjust the repulsive curve to reproduce B3LYP binding energies

	M-M	M-H	M-C	M-N	M-O
M=Sc					
Tier 1	$^1\text{Sc}_2$	$^1\text{ScH}_3$	$^1\text{HScCH}_2$	^1ScN	$^1\text{HScO}$
			$^1\text{H}_2\text{ScCH}_3$	$^1\text{H}_2\text{ScN}_2$	$^1\text{H}_2\text{ScOH}$
M=Ti					
Tier 1	$^1\text{Ti}_2$	$^1\text{TiH}_2$	$^1\text{HTiCH}$	$^1\text{HTiN}$	$^1\text{H}_2\text{TiO}$
			$^1\text{H}_2\text{TiCH}_2$	$^1\text{H}_2\text{TiNH}$	$^1\text{H}_3\text{TiOH}$
			$^1\text{H}_3\text{TiCH}_3$	$^1\text{H}_3\text{TiNH}_2$	
Tier 2			$^1\text{Ti}(\text{CO})_2^{+4}$	$^1\text{Ti}(\text{NH}_3)_2^{+4}$	$^1\text{Ti}(\text{H}_2\text{O})_2^{+4}$
			$^1\text{Ti}(\text{CO})_3^{+4}$	$^1\text{Ti}(\text{NH}_3)_3^{+4}$	$^1\text{Ti}(\text{H}_2\text{O})_3^{+4}$
			$^1\text{Ti}(\text{CO})_4^{+4}$	$^1\text{Ti}(\text{NH}_3)_4^{+4}$	$^1\text{Ti}(\text{H}_2\text{O})_4^{+4}$
			$^1\text{Ti}(\text{CO})_5^{+4}$	$^1\text{Ti}(\text{NH}_3)_5^{+4}$	$^1\text{Ti}(\text{H}_2\text{O})_5^{+4}$
			$^1\text{Ti}(\text{CO})_6^{+4}$	$^1\text{Ti}(\text{NH}_3)_6^{+4}$	$^1\text{Ti}(\text{H}_2\text{O})_6^{+4}$
M=Fe					
Tier 1	$^1\text{Fe}_2$	$^1\text{FeH}_2$	$^1\text{FeCH}_2$	$^1\text{FeNH}$	^1FeO
			$^1\text{FeCH}_3^+$	$^1\text{HFeNH}_2$	$^1\text{HFeOH}$
			$^1\text{HFeCO}$	$^1\text{FeNH}_3^{+2}$	$^1\text{FeOH}_2^{+2}$
Tier 2			$^6\text{Fe}(\text{CO})_2^{+3}$	$^6\text{Fe}(\text{NH}_3)_2^{+3}$	$^6\text{Fe}(\text{H}_2\text{O})_2^{+3}$
			$^6\text{Fe}(\text{CO})_3^{+3}$	$^6\text{Fe}(\text{NH}_3)_3^{+3}$	$^6\text{Fe}(\text{H}_2\text{O})_3^{+3}$
			$^6\text{Fe}(\text{CO})_4^{+3}$	$^6\text{Fe}(\text{NH}_3)_4^{+3}$	$^6\text{Fe}(\text{H}_2\text{O})_4^{+3}$
			$^6\text{Fe}(\text{CO})_5^{+3}$	$^6\text{Fe}(\text{NH}_3)_5^{+3}$	$^6\text{Fe}(\text{H}_2\text{O})_5^{+3}$
			$^6\text{Fe}(\text{CO})_6^{+3}$	$^6\text{Fe}(\text{NH}_3)_6^{+3}$	$^6\text{Fe}(\text{H}_2\text{O})_6^{+3}$
M=Co					
Tier 1	$^1\text{Co}_2$	$^2\text{CoH}_2$	$^1\text{CoCH}$	^1CoN	$^1\text{HCoO}$
		$^1\text{CoH}_3$	$^2\text{CoCH}_2^+$	$^1\text{HCoNH}$	$^1\text{HOCoh}_2$
			$^2\text{CoCO}^{2+}$	$^2\text{CoNH}_3^{+2}$	
Tier 2			$^2\text{Co}(\text{CO})_1^{+2}$	$^2\text{Co}(\text{NH}_3)_1^{+2}$	$^2\text{Co}(\text{H}_2\text{O})_1^{+2}$



M=Ni

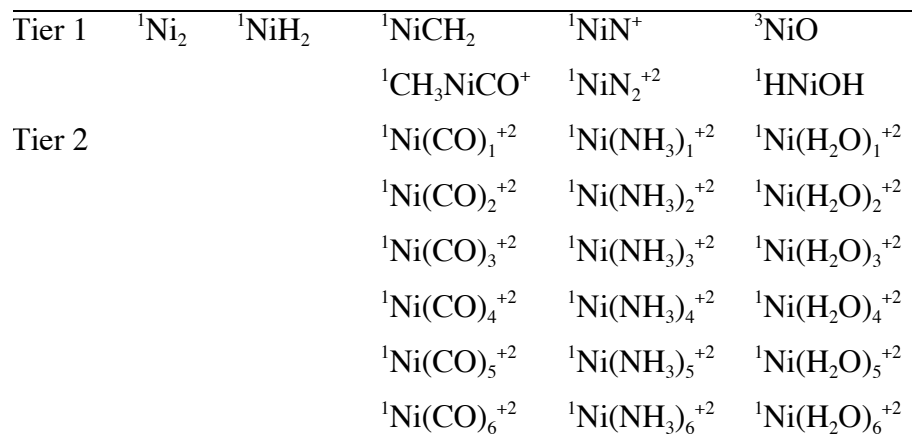


Table 3. DFTB and DFT (B3LYP/SDD+6-31G(d)) optimized bond lengths (Å) and valence angles (°) of Sc-containing Tier 3 molecules, for the geometry parameters defined in Scheme 1

Compound	Multiplicity	Parameter	DFT	SDFTB	Δ
Sc-Sc					
Sc ₂ (CH ₃) ₂	1	r	2.79	2.75	-0.04
		r ₁	2.17	2.18	0.01
		α	109.8	103.1	-6.7
	3	r	2.57	2.76	0.19
		r ₁	2.18	2.18	0.00
		α	180.0	180.0	0.0
Sc ₂ (CH ₃) ₄	1	r	2.81	2.78	-0.03
		r ₁	2.16	2.17	0.01
		α	115.7	106.3	-9.4
	3	r	3.19	2.77	-0.42
		r ₁	2.18	2.19	0.01
		α	121.6	107.9	-13.7
Sc-H					
ScH	1	r	1.74	1.77	0.03
	3	r	1.84	1.83	-0.01
ScH ₂	2	r	1.81	1.81	0.00
		α	118.5	123.6	-5.1
	4	r	1.96	1.90	0.06
		α	180.0	180.0	0.0
Sc ₂ H ₂	1	r	1.96	1.99	0.03
		α	75.4	72.7	-2.7
	3	r	1.97	1.98	0.01
		α	74.1	84.5	-10.4
Sc ₂ H	2	r	1.95	1.98	0.03
		α	73.2	73.8	0.6
	4	r	1.93	1.99	0.06
		α	84.4	87.0	2.6
Sc ₂ H ₄	1	r	1.97	1.99	0.02
		r ₁	1.84	1.83	-0.01
		r ₂	1.97	1.99	0.02
		α	48.7	46.5	-2.2
		α_1	137.7	128.0	-9.7
Sc-C					
Sc(CH ₃) ₂ ⁺	1	r	2.09	2.08	-0.01
		α	104.2	105.1	0.9
	3	r	2.33	2.21	-0.12
		α	113.1	138.8	25.7
Sc(C ₂ H ₄) ⁺	1	r	2.07	2.08	0.01
	3	r	2.36	2.27	-0.11
		r ₁	2.36	2.27	-0.11

CpSc(C ₂ H ₄) ⁺	2	r	2.40	2.30	-0.10
		r ₁	2.40	2.35	-0.05
ScCp ⁺	2	r ₁	2.35	2.30	-0.05
		r ₁	2.35	2.30	-0.05
Sc-N					
Sc(NH ₂) ₂ ⁺	1	r	1.88	1.81	-0.07
		α	176.5	180.0	3.5
	3	r	1.83	1.85	0.02
		α	180.0	180.0	0.0
Sc(NH) ₂	2	r	1.84	1.86	0.02
		α	104.9	115.8	10.9
	4	r	1.96	1.95	-0.01
		α	180.0	180.0	0.0
Sc ⁺ (η ¹ -N ₂)	1	r	2.06	2.02	-0.04
	3	r	2.09	2.04	-0.05
Sc ⁺ (η ² -N ₂)	1	r	2.03	2.04	0.01
	3	r	2.17	2.14	-0.03
Sc-O					
ScO	2	r	1.66	1.67	0.01
	4	r	1.86	1.92	0.06
ScO ₂	2	r	1.77	1.78	0.01
		α	127.1	114.1	-13.0
	4	r	1.92	1.89	-0.03
		α	122.9	79.2	-43.7
Sc(O ₂)	2	r	1.85	1.90	0.05
	4	r	2.11	2.08	-0.03

Table 4. SDFTB and DFT (B3LYP/SDD+6-31G(d)) energies (relative to the respective high-spin states) of the low-lying electronic states of Tier 3 Sc-containing molecules.

Compound	Multi- plicities ^a	Relative Energies (kcal/mol)		
		DFT	SDFTB	Δ
Sc-Sc				
Sc ₂ (CH ₃) ₂	3→1	7.2	-13.0	20.3
Sc ₂ (CH ₃) ₄	3→1	-9.5	-15.3	5.8
Sc-H				
ScH	3→1	-4.3	-2.1	2.2
ScH ₂	4→2	-87.6	-63.0	24.7
Sc ₂ H ₂	3→1	6.7	0.3	-4.4
Sc ₂ H	4→2	8.8	-29.4	-38.2
Sc ₂ H ₄	3→1	-3.8	-5.4	-1.6
Sc-C				
Sc(CH ₃) ₂ ⁺	3→1	-51.4	-62.4	-10.9
Sc(C ₂ H ₄) ⁺	3→1	-1.4	-24.0	-22.6
ScCp ⁺	4→2	-74.1	-65.6	8.5
Sc-N				
Sc(NH ₂) ₂ ⁺	3→1	-49.2	-71.2	-22.1
Sc(NH) ₂	4→2	-45.7	-71.5	-25.8
Sc ⁺ (η^1 -N ₂)	3→1	21.5	11.6	-10.0
Sc ⁺ (η^2 -N ₂)	3→1	5.9	-8.7	-14.6
Sc-O				
ScO	4→2	-76.8	-94.5	17.7
ScO ₂	4→2	-58.5	-86.2	27.7
Sc(O ₂)	4→2	-43.9	-44.7	-0.8

^a For instance, 3→1 means that the energy of the singlet (low spin) state relative to the triplet (high spin) state.

Table 5. SDFTB and DFT (B3LYP/SDD+6-31G(d)) optimized bond lengths (Å) and valence angles (°) of Ti-containing Tier 3 molecules, for the geometry parameters defined in Scheme 1

Compound	Multiplicity	Parameter	DFT	SDFTB	Δ
Ti-H					
TiH	2	r	1.68	1.74	0.06
	4	r	1.84	1.76	-0.08
TiH ₂	1	r	1.75	1.71	-0.04
		α	106.9	111.9	5.0
	3	r	1.78	1.74	-0.04
		α	122.3	108.3	-14.0
Ti ₂ H	2	r	1.86	1.89	0.03
		α	102.0	64.6	-37.4
	4	r	1.82	1.93	0.11
		α	83.0	75.1	-7.9
Ti ₂ H ₂	1	r	1.86	1.80	-0.06
		α	48.3	57.8	9.5
	3	r	1.87	1.88	0.01
		α	57.2	57.3	0.1
Ti ₂ H ₄	1	r	1.85	1.87	0.02
		r ₁	1.74	1.75	0.01
		α	58.0	55.2	-2.8
Ti-C					
Ti(CH ₃) ₂	1	r	2.04	2.05	0.01
		α	110.7	112.5	1.8
	3	r	2.18	2.08	-0.10
		α	117.1	114.8	-2.3
Ti(C ₂ H ₄) ⁺	2	r	2.03	2.00	-0.03
	4	r	2.34	2.26	-0.08
TiCp ⁺	1	r ₁	2.26	2.20	-0.06
	3	r ₁	2.27	2.27	0.00
Ti-N					
Ti(NH ₂) ₂ ⁺	2	r	1.85	1.84	-0.01
		α	118.3	115.1	-3.2
Ti(NH) ₂	1	r	1.71	1.70	-0.01
		α	114.8	117.7	3.1
Ti ⁺ (η^1 -N ₂)	2	r	1.99	2.00	0.01
Ti-O					
TiO	1	r	1.59	1.59	0.00
	3	r	1.61	1.61	0.00
Ti ₂ O ₂	1	r	1.81	1.91	0.10
		α	51.4	52.0	0.6
TiO ₂	1	r	1.64	1.64	0.00
		α	117.7	111.5	-6.2
Ti(O ₂)	1	r	1.79	1.81	0.02

Ti ₂ O ₄	1	α	49.3	56.4	7.1
		r	1.84	1.84	0.00
		r ₁	1.63	1.63	0.00
		α	42.6	47.7	5.1

Table 6. SDFTB and DFT (B3LYP/SDD+6-31G(d)) energies (relative to the respective high-spin states) of the low-lying electronic states of Tier 3 Ti-containing molecules.

Compound	Multi- plicities ^a	Relative Energies (kcal/mol)		
		DFT	SDFTB	Δ
Ti-H				
TiH	4→2	1.2	19.7	18.5
TiH ₂	3→1	39.8	14.2	-25.6
Ti ₂ H ₂	3→1	2.1	-10.0	-12.1
Ti ₂ H ₄	3→1	24.9	45.8	20.9
Ti-C				
Ti(CH ₃) ₂	3→1	5.9	12.7	6.8
Ti(C ₂ H ₄) ⁺	4→2	8.2	-3.6	-11.8
TiCp ⁺	3→1	12.0	13.6	1.6
Ti-O				
TiO	3→1	31.4	6.4	-25.0

^aFor instance, 3→1 means that the energy of the singlet (low spin) state relative to the triplet (high spin) state.

Table 7. SDFTB and DFT (B3LYP/SDD+6-31G(d)) optimized bond lengths (Å) and valence angles (°) of Fe-containing Tier 3 molecules, for the geometry parameters defined in Scheme 1

Compound	Multiplicity	Parameter	DFT	SDFTB	Δ
Fe-H					
FeH	2	r	1.59	1.50	-0.09
	4	r	1.56	1.54	-0.02
FeH ₂	3	r	1.54	1.51	-0.03
		α	102.4	96.9	-5.5
	5	r	1.65	1.62	-0.03
		α	169.7	153.0	-16.7
Fe ₂ H	2	r	1.68	1.66	0.02
		α	46.45	50.79	4.34
Fe ₂ H ₄	1	r	1.52	1.52	0.00
		r ₁	1.65	1.49	0.16
		α	46.79	63.9	17.11
Fe ₂ H ₄	3	r	1.58	1.60	0.02
		r ₁	1.61	1.72	0.11
		α	47.27	48.87	1.60
Fe-C					
Fe(CH ₃) ₂	1	r	1.92	2.06	0.14
		α	117.7	112.2	-5.5
	3	r	1.94	2.07	0.13
		α	112.1	109.3	-2.8
	5	r	2.05	2.13	0.08
		α	180.0	180.0	0.0
Fe(C ₂ H ₄) ⁺¹	2	r	2.05	2.13	0.08
	4	r	2.07	2.18	0.11
FeCp ⁺¹	3	r ₁	2.19	2.26	0.07
	5	r ₁	2.23	2.32	0.09
Fe-N					
Fe(NH ₂) ₂	1	r	1.79	1.76	0.03
		α	180.0	150.7	-29.3
	5	r	1.85	1.86	0.01
		α	180.0	180.0	0.0
Fe(NH) ₂	3	r	1.65	1.60	-0.05
		α	171.2	180.0	8.8
	5	r	1.67	1.76	0.09
		α	121.1	142.1	21.0
Fe(η^1 -N ₂) ⁺¹	4	r	2.09	1.92	-0.17
		α	0.00	0.01	0.01
Fe-O					
FeO	1	r	1.59	1.58	-0.01
	3	r	1.57	1.61	0.04
	5	r	1.61	1.66	0.05

Fe ₂ O ₂	1	r	1.73	1.80	0.07
		α	42.8	51.8	9.0
	3	r	1.76	1.81	0.05
		α	42.8	52.6	9.8
FeO ₂	1	r	1.54	1.61	0.07
		α	145.2	167.6	22.4
	3	r	1.58	1.63	0.05
		α	140.4	149.4	9.0
	5	r	1.60	1.67	0.07
		α	118.7	126.0	7.3
Fe(O ₂) ⁺¹	4	r	1.82	1.81	-0.01
		α	43.8	44.1	0.3
Fe ₂ O ₄	1	r ₁	1.56	1.57	0.01
		r	1.72	1.81	0.09
		α	47.6	44.4	-3.2
	3	r ₁	1.53	1.59	0.06
		r	1.74	1.80	0.06
		α	43.9	45.4	1.5

Table 8. SDFTB and DFT (B3LYP/SDD+6-31G(d)) energies (relative to the respective high-spin states) of the low-lying electronic states of Tier 3 Fe-containing molecules.

Compound	Multi-plicities ^a	Relative Energies (kcal/mol)		
		DFT	SDFTB	Δ
Fe-H				
FeH	4→2	43.7	33.5	-10.2
FeH ₂	3→1	22.0	11.7	-10.3
Fe-C				
Fe(CH ₃) ₂	3→1	33.1	19.7	-13.4
Fe(C ₂ H ₄) ⁺¹	4→2	41.6	32.4	-9.2
FeCp ⁺¹	5→3	13.8	16.7	2.9
Fe-N				
Fe(NH ₂) ₂	5→1	33.3	12.4	-20.9
Fe(NH) ₂	5→3	8.2	27.6	19.4
Fe(η^1 -N ₂)	4→2	25.5	37.1	11.6
Fe-O				
FeO	5→1	10.6	0.6	-10.0
Fe ₂ O ₂	3→1	40.4	6.0	-34.4
FeO ₂	3→1	26.4	8.0	-18.4
Fe(O ₂) ⁺¹	4→2	47.1	14.0	-33.1
Fe ₂ O ₄	3→1	7.0	0.7	-6.3

^a For instance, 3→1 means that the energy of the singlet (low spin) state relative to the triplet (high spin) state.

Table 9. SDFTB and DFT (B3LYP/SDD+6-31G(d)) optimized bond lengths (Å) and valence angles (°) of Co-containing Tier 3 molecules, for the geometry parameters defined in Scheme 1

Compound	Multiplicity	Parameter	DFT	SDFTB	Δ
Co-H					
CoH	1	r	1.54	1.52	-0.02
	3	r	1.54	1.52	-0.02
CoH ₂	2	r	1.49	1.47	-0.02
		α	97.4	93.9	-3.5
	4	r	1.59	1.58	-0.01
		α	143.2	140.3	-2.9
Co ₂ H ₂	1	r	1.62	1.63	0.01
		α	48.4	47.1	-1.3
	3	r	1.63	1.64	0.01
		α	47.5	47.8	0.3
Co(CH ₃) ₂	2	r	1.89	1.99	0.10
		α	114.0	106.2	-7.8
	4	r	1.99	2.04	0.05
		α	143.9	146.8	2.9
Co(C ₂ H ₄) ⁺²	4	r	2.30	2.08	-0.22
	6	r	2.19	2.06	-0.13
CoCp ⁺¹	4	r ₁	1.80	1.79	-0.01
	6	r ₁	2.30	2.52	0.22
Co-N					
Co(NH ₂) ₂	4	r	1.82	1.80	-0.02
		α	179.9	179.4	-0.5
	6	r	1.90	1.84	-0.06
		α	97.0	96.3	-0.7
Co(NH) ₂ linear	4	r	1.68	1.66	-0.02
		α	180.0	180.0	0.0
	6	r	1.78	1.73	-0.05
		α	179.1	180.0	0.9
Co(NH) ₂ bent	4	r	1.67	1.65	-0.02
		α	128.4	127.0	1.4
	6	r	1.75	1.72	-0.03
		α	127.8	142.0	13.6
Co ²⁺ (η^1 -N ₂)	2	r	2.00	1.95	-0.05
	4	r	1.99	1.98	-0.01
Co-O					
CoO	2	r	1.60	1.58	-0.02
	4	r	1.59	1.61	0.02
Co ₂ O ₂	1	r	1.73	1.77	0.04
		α	45.9	42.6	-3.3
	3	r	1.74	1.78	0.04
		α	44.2	45.1	0.9

CoO ₂ linear	2	r	1.57	1.57	0.00
		α	177.7	179.5	1.8
CoO ₂ bent	4	r	1.64	1.63	-0.01
		α	101.4	116.7	15.3
Co(O ₂)	4	r	1.81	1.83	0.02
		α	47.9	44.7	3.2
	6	r	2.03	1.92	-0.11
		α	38.1	40.3	2.2
Co ₂ O ₄	1	r ₁	1.53	1.55	0.02
		r	1.75	1.78	0.03
		α	43.5	42.8	-0.7
	3	r ₁	1.53	1.56	0.03
		r	1.76	1.78	0.02
		α	44.7	41.7	-3.0
	5	r ₁	1.56	1.59	0.03
		r	1.75	1.78	0.03

Table 10. SDFTB and DFT (B3LYP/SDD+6-31G(d)) energies (relative to the respective high-spin states) of the low-lying electronic states of Tier 3 Co-containing molecules.

Compound	Multi- plicities ^a	Relative Energies (kcal/mol)		
		DFT	SDFTB	Δ
Co-H				
CoH	3→1	54.3	18.2	-36.1
CoH ₂	4→2	11.2	-11.2	-22.4
Co ₂ H ₂	3→1	25.3	10.5	-14.8
Co-C				
Co(CH ₃) ₂	4→2	9.2	-1.1	-10.3
Co(C ₂ H ₄) ⁺²	6→4	81.6	95.8	14.2
CoCp ⁺¹	6→4	21.8	46.0	24.2
Co-N				
Co(NH ₂) ₂	6→4	-57.7	-74.0	-16.3
Co(NH) ₂ bent	6→4	-8.8	-33.8	-25.0
Co(NH) ₂ linear	6→4	6.7	49.0	42.3
Co ²⁺ (η^1 -N ₂)	4→2	28.4	22.0	-6.4
Co-O				
CoO	4→2	39.7	7.8	-31.9
Co ₂ O ₂	3→1	5.3	1.1	-4.2
Co(O ₂)	6→4	5.2	-26.8	-32.0
Co ₂ O ₄	3→1	29.7	3.0	-26.7

^a For instance, 3→1 means that the energy of the singlet (low spin) state relative to the triplet (high spin) state.

Table 11. SDFTB and DFT (B3LYP/SDD+6-31G(d)) optimized bond lengths (Å) and valence angles (°) of Ni-containing Tier 3 molecules, for the geometry parameters defined in Scheme 1

Compound	Multiplicity	Parameter	DFT	SDFTB	Δ
Ni-Ni					
Ni ₂ (CH ₃) ₂	1	r	2.19	2.22	0.03
		r ₁	1.85	1.97	0.12
		α	97.3	96.9	0.4
	3	r	2.35	2.16	0.19
		r ₁	1.91	2.01	0.10
		α	132.5	114.6	17.9
Ni ₂ (CH ₃) ₄	1	r	2.46	2.24	0.22
		r ₁	1.86	1.98	0.12
		α	120.0	109.2	10.8
	3	r	2.30	2.16	0.14
		r ₁	1.94	2.08	0.14
		r ₂	1.91	2.08	0.17
		r ₃	2.08	2.08	0.00
		α_1	121.0	114.1	6.9
		α_2	121.1	114.1	7.0
		α_3	60.1	114.1	54.0
Ni-H					
NiH	2	r	1.51	1.46	-0.05
	4	r	1.60	1.60	0.00
NiH ₂	1	r	1.53	1.54	0.00
		α	180.0	180.0	0.0
	3	r	1.54	1.52	-0.03
		α	131.9	136.8	4.9
Ni ₂ H ₂	1	r	1.57	1.59	0.02
		α	41.4	45.1	3.3
	3	r	1.67	1.57	-0.10
		α	49.6	43.4	-6.2
Ni-C					
Ni(CH ₃) ₂ ⁺	1	r	1.94	2.04	0.10
		α	180.0	180.0	0.0
	3	r	1.96	2.03	0.06
		α	139.3	142.6	3.3
Ni(C ₂ H ₄) ⁺	2	r	2.08	2.15	0.07
	4	r	2.32	2.28	-0.04
NiCp ⁺		r ₁	2.85	3.08	0.23
	1	r ₁	1.71	2.19	0.48
	3	r ₁	1.77	1.90	0.13
Ni-N					
Ni(NH ₂) ₂ ⁺	2	r	1.88	1.81	-0.07
		α	176.5	180.0	3.6

	4	r	1.83	1.85	0.02
		α	180.0	180.0	0.0
Ni(NH) ₂	1	r	1.60	1.66	0.06
		α	164.9	180.0	15.1
	3	r	1.67	1.72	0.05
		α	125.4	170.6	45.2
Ni ⁺ (η^1 -N ₂)	2	r	1.91	1.94	0.03
	4	r	2.44	2.17	-0.27
Ni-O					
NiO	1	r	1.61	1.62	0.01
	3	r	1.61	1.62	0.01
Ni ₂ O ₂	1	r	1.75	1.79	0.04
		α	50.2	52.1	1.9
	3	r	1.77	1.78	0.01
		α	47.9	50.3	2.4
NiO ₂	1	r	1.58	1.58	0.00
		α	159.4	180.0	30.6
	3	r	1.60	1.61	0.01
		α	132.7	142.0	10.7
Ni(O ₂)	1	r	1.78	1.79	0.01
	3	r	1.90	1.83	-0.07
Ni ₂ O ₄	1	r	1.76	1.78	0.02
		r ₁	1.58	1.59	0.01
		α	42.7	41.2	-1.5

Table 12. SDFTB and DFT (B3LYP/SDD+6-31G(d)) energies (relative to the respective high-spin states) of the low-lying electronic states of Tier 3 Ni-containing molecules.

Compound	Multi- plicities ^a	Relative Energies (kcal/mol)		
		DFT	SDFTB	Δ
Ni-Ni				
Ni ₂ (CH ₃) ₂	3→1	19.5	-3.8	23.3
Ni ₂ (CH ₃) ₄	3→1	14.0	-8.4	22.4
Ni-H				
NiH	4→2	-26.3	-47.0	20.7
NiH ₂	3→1	33.8	12.0	21.8
Ni ₂ H ₂	3→1	28.6	-20.0	48.6
Ni-C				
Ni(CH ₃) ₂ ⁺	3→1	35.9	10.4	25.5
Ni(C ₂ H ₄) ⁺	4→2	-39.9	-45.9	5.8
NiCp ⁺	3→1	21.2	-9.0	30.2
Ni-N				
Ni(NH ₂) ₂ ⁺	4→2	10.4	-7.3	17.7
Ni(NH) ₂	3→1	-7.2	-29.6	22.4
Ni ⁺ (η ¹ -N ₂)	4→2	-37.5	-57.0	19.5
Ni-O				
NiO	3→1	47.1	12.8	-34.3
Ni ₂ O ₂	3→1	29.9	1.4	-28.5
NiO ₂	3→1	2.7	-14.0	-16.7
Ni(O ₂)	3→1	11.9	-10.7	-22.6

^a For instance, 3→1 means that the energy of the singlet (low spin) state relative to the triplet (high spin) state.

Figure Captions

Scheme 1. Schematic representation of the geometrical parameters of the set of Tier 3 molecules for M = Ti, Fe, Co and Ni. For symmetric structures, only the unique parameters are given.

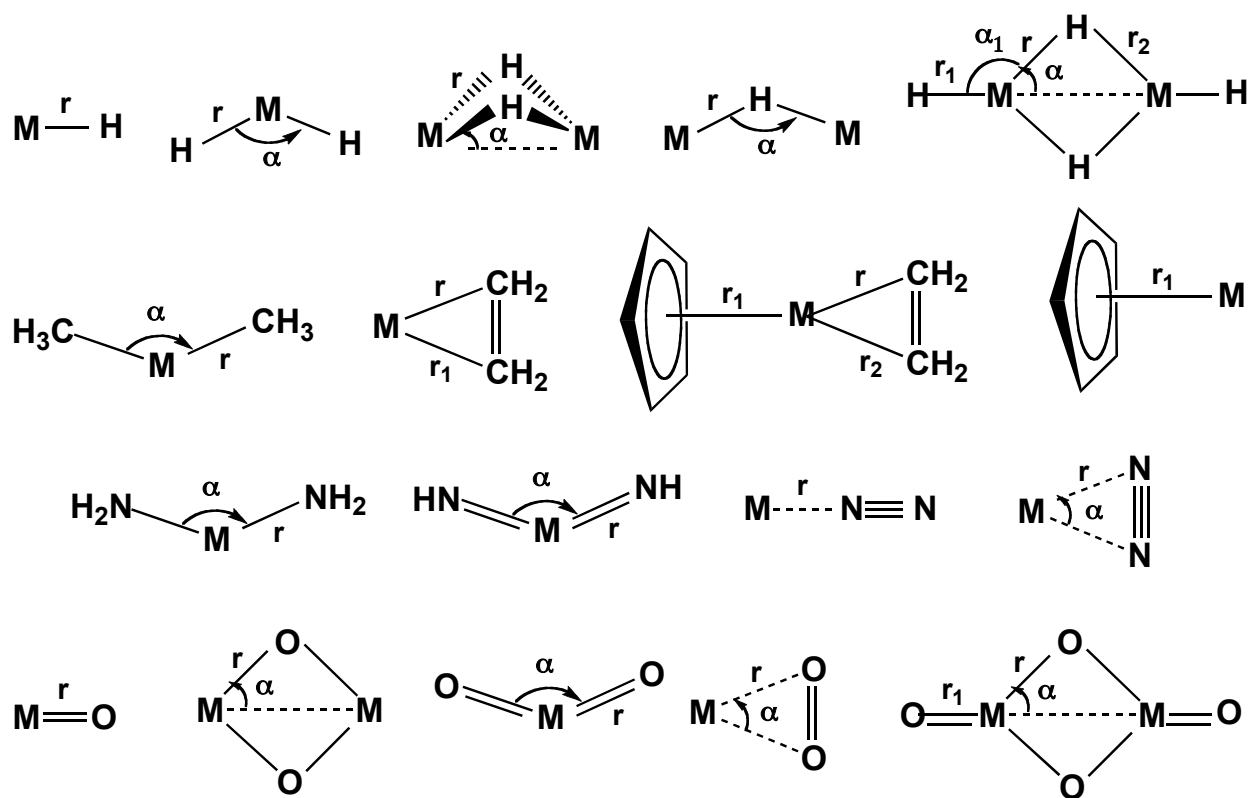
Figure 1. B3LYP/6-311+G(d) and SDFTB optimized bond distances (in Å) and Sc-C binding energies (in kcal/mol) for the electronic 2S ground state of $Sc(CC)_n$ species, $n=1-4$. Italic and plain values denote the DFT and SDFTB results, respectively.

Figure 2. B3LYP/SDD+6-31G(d) (upper numbers) and SDFTB (lower numbers) optimized geometries (distances in Å) and energetics (in kcal/mol) of the reactant, intermediates and product of the reaction $[(Cp-CH_2-Cp)TiCH_3]^+ + C_2H_4 \rightarrow [(Cp-CH_2-Cp)Ti(CH_2CH_2CH_3)]^+$

Figure 3. B3LYP/SDD+6-31G(d) (upper numbers) and SDFTB (lower numbers) optimized geometries (distances in Å) for the CO complex of Fe-phorphyrin.

Figure 4. B3LYP/SDD+6-31G(d) (upper numbers) and SDFTB (lower numbers) optimized geometries (distances in Å) geometries of adenosylcobalamin and methylcobalamin.

Figure 5. B3LYP/Lan12DZ (upper numbers) and SDFTB (lower numbers) optimized geometries (distances in Å) and energetics (in kcal/mol) of the reactant, intermediates and product of the ethylene insertion step of ethylene polymerization: $[(NHCHCHNH)NiCH_3]^+ + CH_2=CH_2 \rightarrow [(NHCHCHNH)NiCH_2CH_2CH_3]^+$



Scheme 1. Schematic representation of the geometrical parameters of the set of Tier 3 molecules for $M = Ti, Fe, Co$ and Ni . For symmetric structures, only the unique parameters are given.

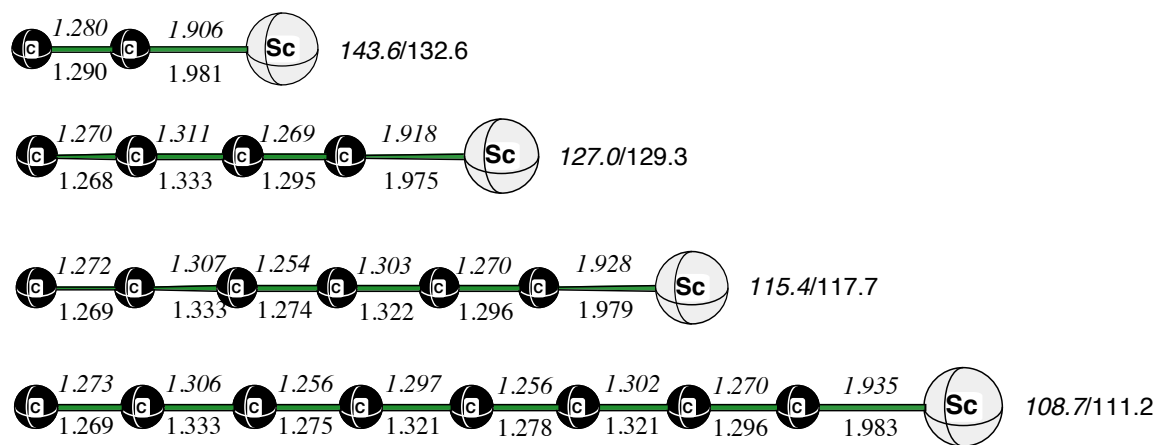


Figure 1. B3LYP/6-311+G(d) and SDFTB optimized bond distances (in Å) and Sc-C binding energies (in kcal/mol) for the electronic 2S ground state of $Sc(CC)_n$ species, $n=1-4$. Italic and plain values denote the DFT and SDFTB results, respectively.

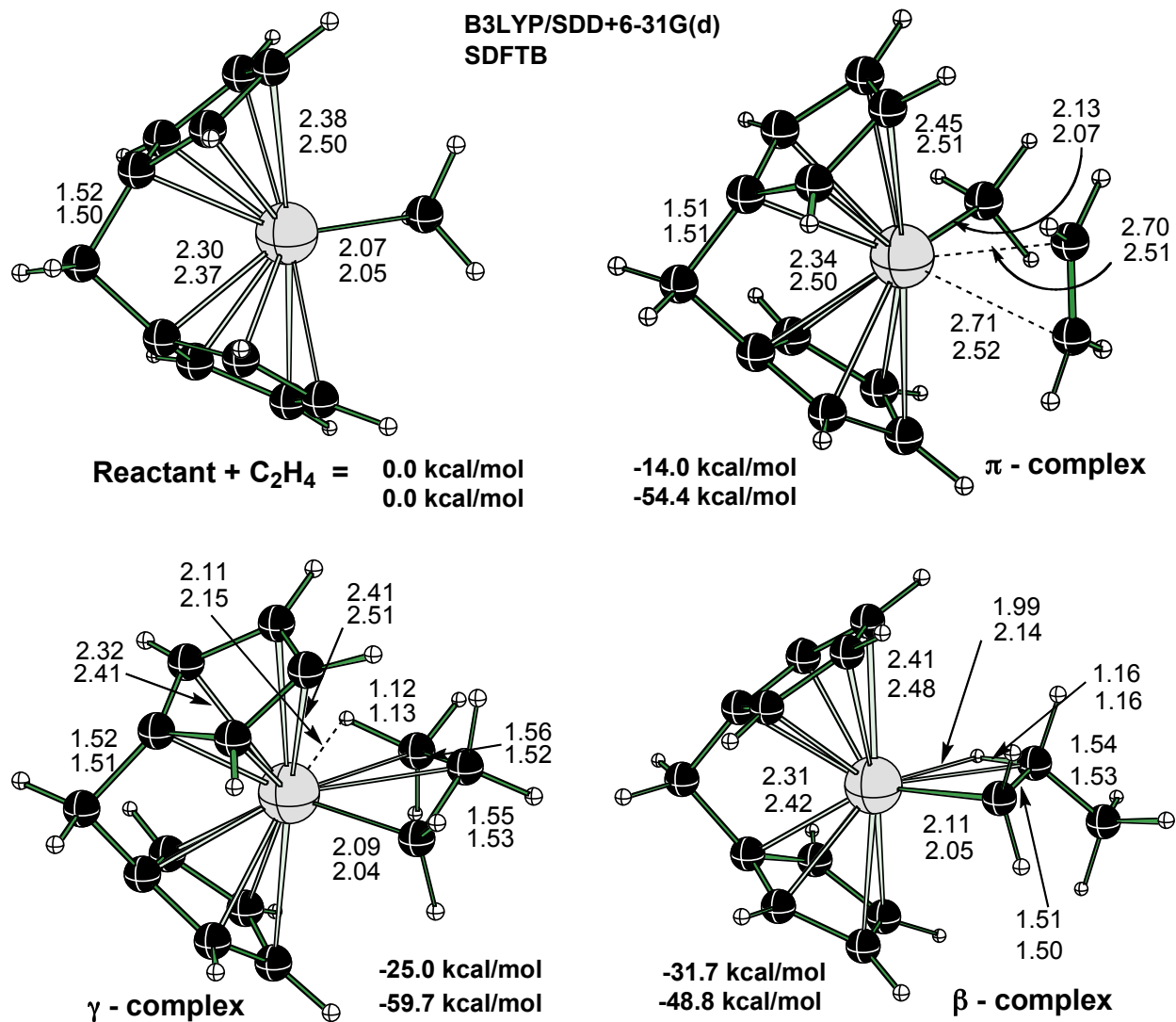


Figure 2. B3LYP/SDD+6-31G(d) (upper numbers) and SDFTB (lower numbers) optimized geometries (distances in Å) and energetics (in kcal/mol) of the reactant, intermediates and product of the reaction $[(\text{Cp-CH}_2\text{-Cp})\text{TiCH}_3]^+ + \text{C}_2\text{H}_4 \rightarrow [(\text{Cp-CH}_2\text{-Cp})\text{Ti}(\text{CH}_2\text{CH}_2\text{CH}_3)]^+$

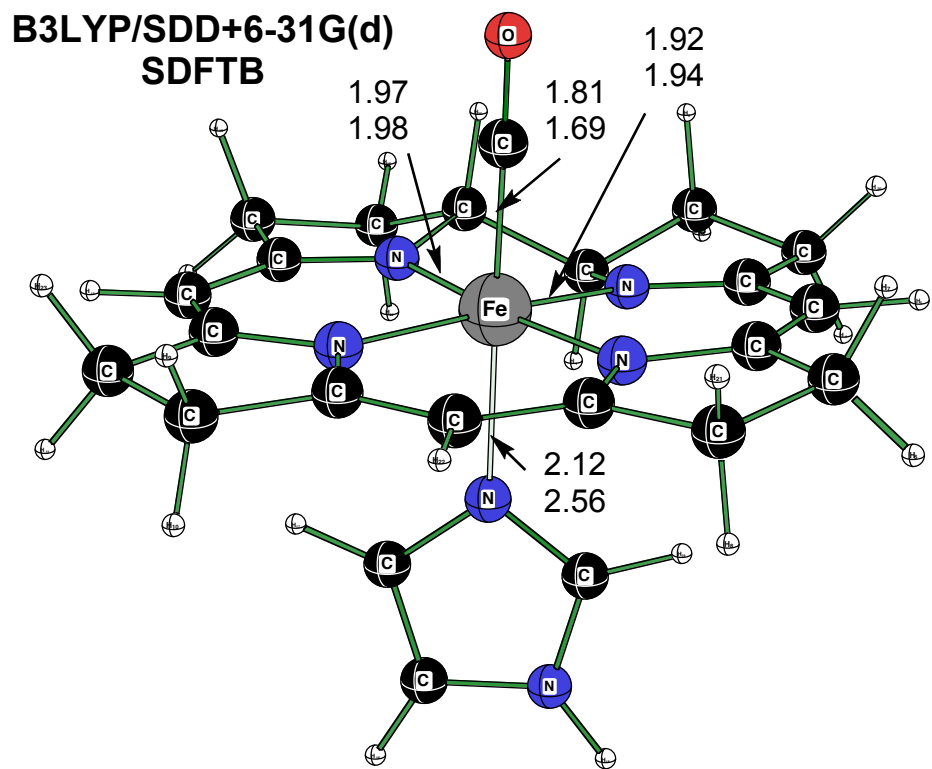


Figure 3. B3LYP/SDD+6-31G(d) (upper numbers) and SDFTB (lower numbers) optimized geometries (distances in Å) for the CO complex of Fe-porphyrin.

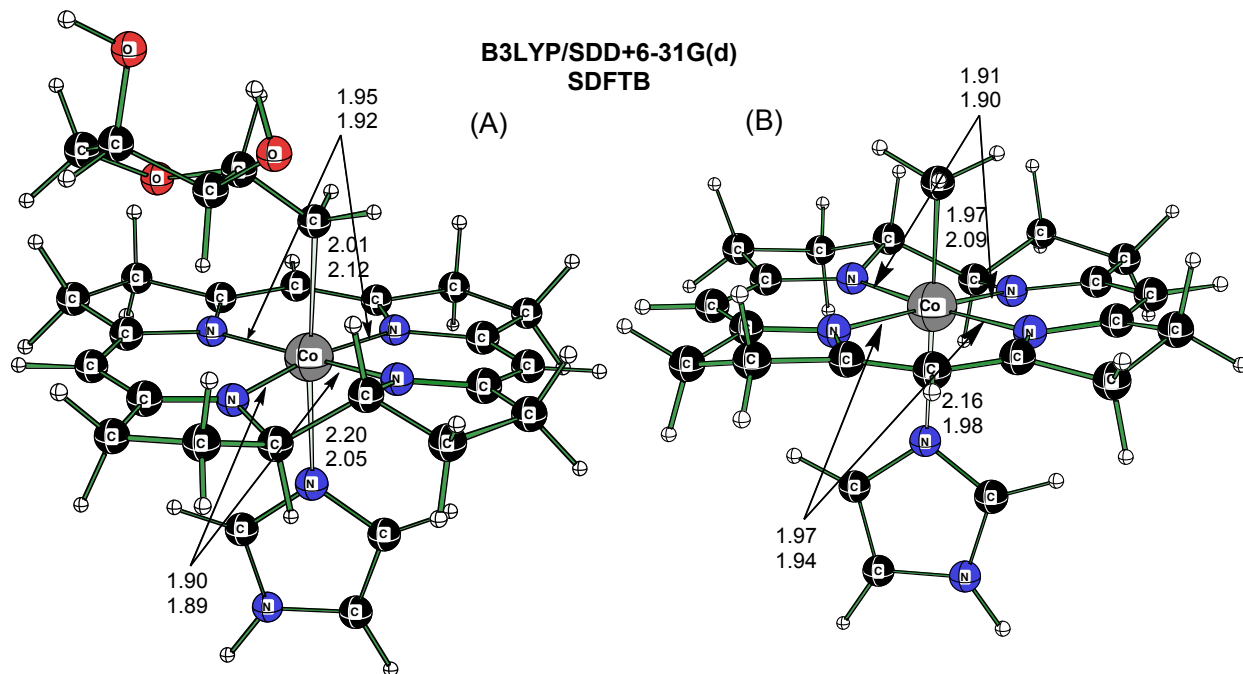


Figure 4. B3LYP/SDD+6-31G(d) (upper numbers) and SDFTB (lower numbers) optimized geometries (distances in Å) geometries of (A) adenosylcobalamin and (B) methylcobalamin.

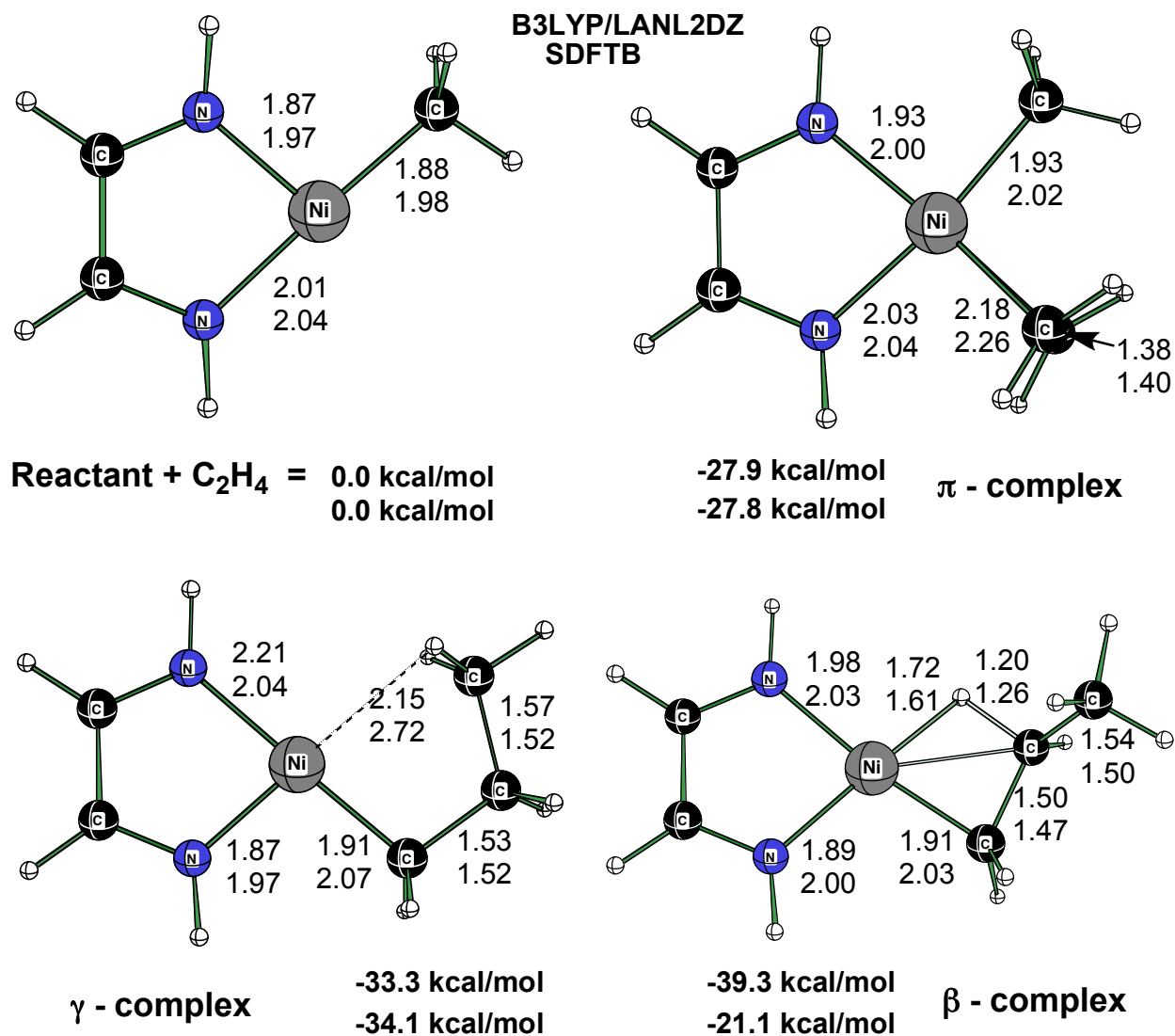


Figure 5. B3LYP/Lanl2DZ (upper numbers) and SDFTB (lower numbers) optimized geometries (distances in Å) and energetics (in kcal/mol) of the reactant, intermediates and product of the ethylene insertion step of ethylene polymerization: $[(\text{NHCHCHNH})\text{NiCH}_3]^+ + \text{CH}_2=\text{CH}_2 \rightarrow [(\text{NHCHCHNH})\text{NiCH}_2\text{CH}_2\text{CH}_3]^+$